Supporting Information for:

Paired Agent Fluorescence Imaging of Cancer in a Living Mouse Using Pre-assembled Squaraine Molecular Probes with Emission Wavelengths of 690 and 830 nm.

Cynthia L. Schreiber, Canjia Zhai, Janel M. Dempsey, Hannah H. McGarraugh, Braden P. Matthews, Caroline R. Christmann, and Bradley D. Smith*

Department of Chemistry and Biochemistry, 251 Nieuwland Science Hall, University of Notre Dame, Notre Dame, Indiana 46556, USA

*E-mail: smith.115@nd.edu

Contents

A. Synthesis and Characterization

Materials and Equipment

All chemicals and solvents were purchased as reagent grade and used without further purification unless otherwise noted. Reactions were monitored by analytical thin-layer chromatography (TLC) on silica gel 60-F_{254} plates, visualized by ultraviolet (254, 365 nm) or $KMnO_4$ stain. ^1H NMR spectra were recorded on Bruker AVANCE III HD 400 or 500 MHz spectrometer at 25 °C. Chemical shift was presented in ppm and referenced by residual solvent peak. Mass spectrometry (MS) was performed using a Bruker micro TOP II spectrometer. Flash column chromatography was performed using silica gel (silicaFlash P60 from SILICYCLE).

Synthesis

The syntheses of macrocycle **C**,[S1] squaraines **SQ690-P3**,[S2] **SQ690-P45**,[S2] and **SQ830-P45**[S3] were previously reported and were confirmed by NMR, mass spectrometry, UV/Vis, and fluorescence spectroscopy.

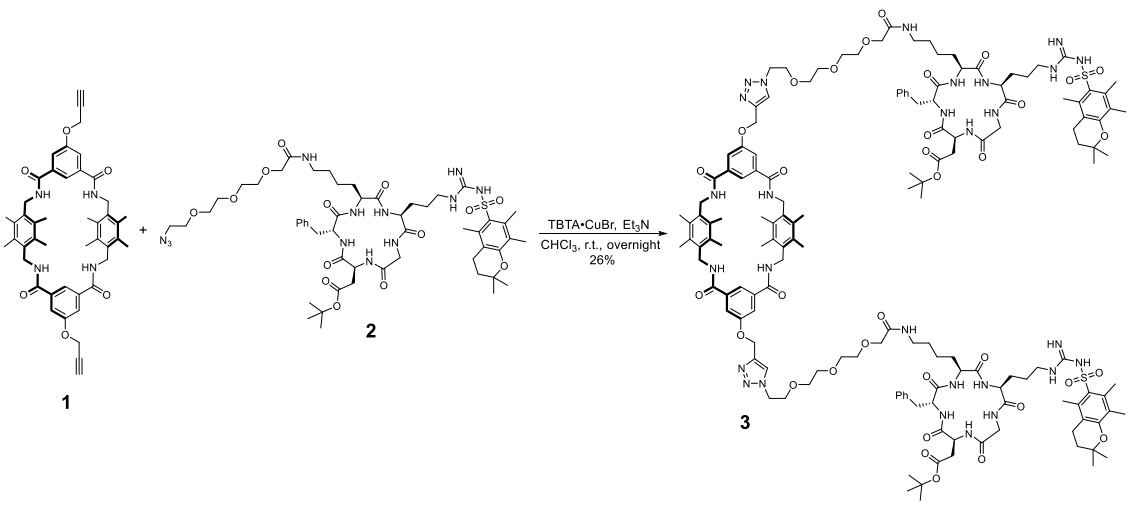

Compound **3**.

Compound **1**[S1] and compound **2**[S4] were synthesized according to previously reported procedures. Compound **1** (4.4 mg, 0.00584 mmol) was added into a solution of **2** (13.6 mg, 0.0117 mmol) in $CHCl_3$ (2 mL). Triethylamine (30 μL) and TBTA•CuBr (4 mg) were added into the mixture. The reaction was stirred at room temperature overnight. The reaction mixture was filtered, and the solution was collected. Solvent was removed by rotary evaporation, and the residue was purified by column chromatography (0-20% MeOH in $CHCl_3$) to yield product **3** as light-yellow solid (4.6 mg, 26%). **^{1}H NMR** (500 MHz, Methanol-d_4) δ 8.20 (s, 2H), 7.82 – 7.77 (m, 4H), 7.66 (s, 2H), 7.22 (dd, *J* = 25.7, 7.1 Hz, 10H), 5.31 (s, 4H), 5.12 (d, *J* = 1.2 Hz, 3H), 4.71 (dd, *J* = 8.1, 6.4 Hz, 2H), 4.61 (s, 8H), 4.57 (d, *J* = 8.0 Hz, 2H), 4.19 (d, *J* = 15.3 Hz, 4H), 4.01 – 3.94 (m, 3H), 3.94 – 3.87 (m, 7H), 3.67 – 3.54 (m, 19H), 3.34 (s, 4H), 3.11 (dd, *J* = 15.0, 7.7 Hz, 6H), 2.96 (q, *J* = 8.2, 6.6 Hz, 3H), 2.72 (dd, *J* = 16.0, 8.2 Hz, 2H), 2.61 (t, *J* = 6.7 Hz, 4H), 2.49 (t, *J* = 6.8 Hz, 12H), 2.22 (s, 13H), 2.06 (s, 4H), 1.79 (t, *J* = 6.9 Hz, 4H), 1.62 (d, *J* = 19.7 Hz, 6H), 1.53 – 1.43 (m, 8H), 1.40 (s, 17H), 1.34 – 1.26 (m, 71H), 1.17 (t, *J* = 7.0 Hz, 6H), 1.02 (s, 5H), 0.90 (t, *J* = 6.7 Hz, 10H).

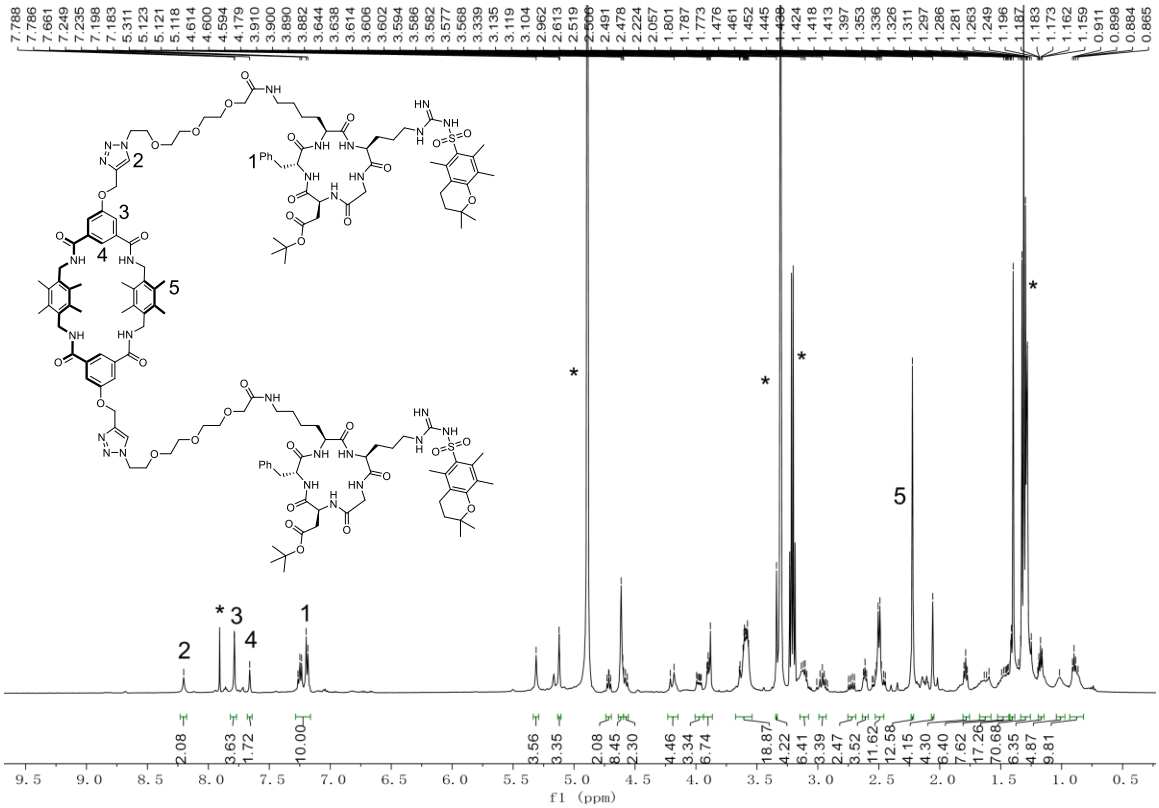

Figure S1. Compound **3** ^{1}H NMR spectrum (500 MHz, CD_3OD). (*: Solvent peak residue; *NH* peaks exchanged with CD_3OD)

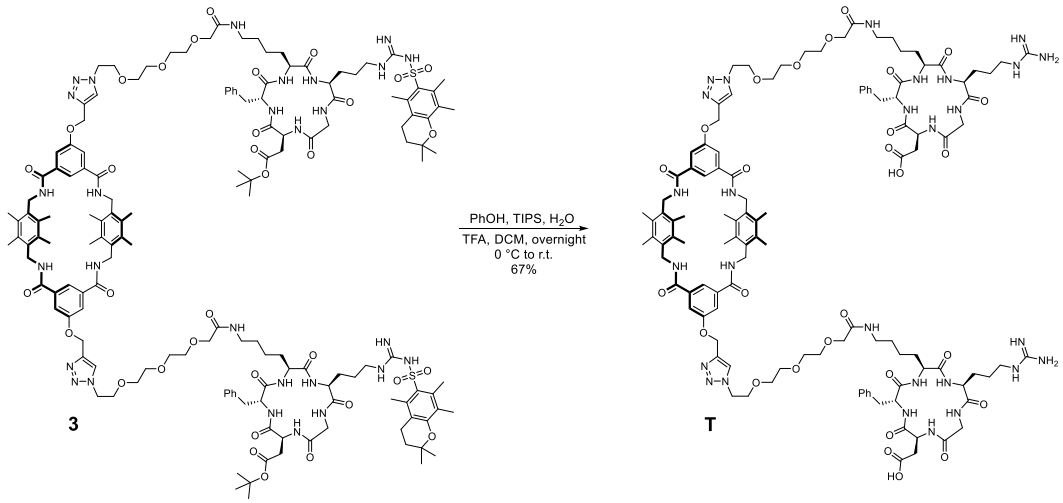

Compound **T**.

Triisopropylsilane (200 μL), H_2O (200 μL) and phenol (50 mg) were added into a solution of compound **3** (4.6 mg, 0.00152 mmol) in dichloromethane (2 mL). The mixture was then put into ice bath. Trifluoroacetic acid (2 mL) was added dropwise into the mixture. The reaction was then stirred at room temperature overnight. Solvent was removed by rotary

evaporation and the residue was washed with diethyl ether to yield product **T** as light yellow solid (2.4 mg, 67%). **^{1}H NMR** (500 MHz, Methanol-d_4) δ 8.21 (s, 2H), 7.79 (d, *J* = 1.3 Hz, 4H), 7.66 (s, 2H), 7.28 – 7.16 (m, 10H), 5.32 (s, 4H), 4.75 (t, *J* = 7.1 Hz, 4H), 4.63 (d, *J* = 10.1 Hz, 8H), 4.54 (t, *J* = 7.8 Hz, 4H), 4.28 – 4.22 (m, 5H), 3.98 – 3.89 (m, 9H), 3.67 – 3.58 (m, 14H), 3.44 (p, *J* = 1.7 Hz, 2H), 3.34 – 3.32 (m, 2H), 3.23 (dd, *J* = 14.0, 7.2 Hz, 6H), 3.18 – 3.08 (m, 8H), 2.97 (dd, *J* = 7.7, 4.9 Hz, 4H), 2.81 (dd, *J* = 16.4, 8.1 Hz, 4H), 2.56 (dd, *J* = 16.5, 6.3 Hz, 4H), 2.25 (s, 24H), 1.92 – 1.83 (m, 5H), 1.67 (s, 6H), 1.59 – 1.44 (m, 10H), 1.41 – 1.33 (m, 5H), 1.32 – 1.28 (m, 2H), 1.09 – 0.95 (m, 10H). **HRMS (ESI-TOF)**: calculated for $C_{116}H_{157}N_{28}O_{28}^+$ $[M+H]^+$ 2391.1750, found 2391.1520.

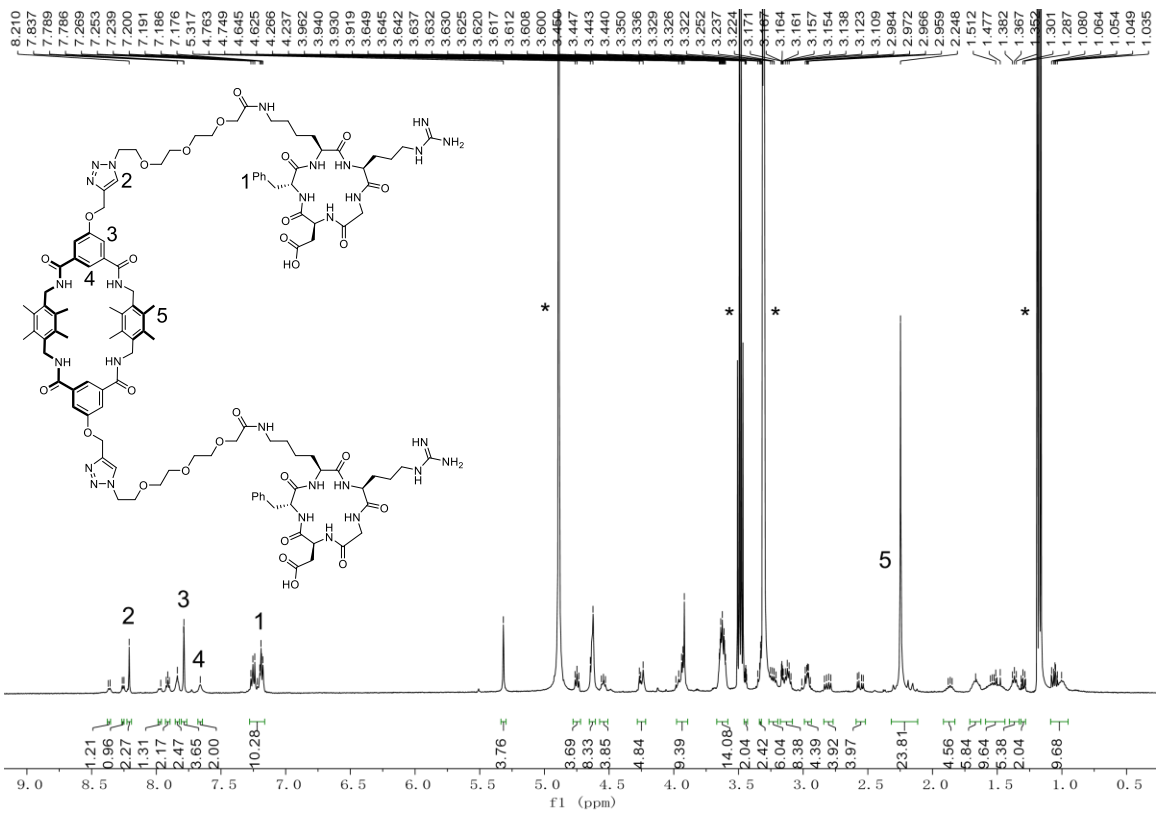

Figure S2. Compound **T** ^{1}H NMR spectrum (500 MHz, CD_3OD). (*: Solvent peak residue; *NH* peaks not completely exchanged with CD_3OD)

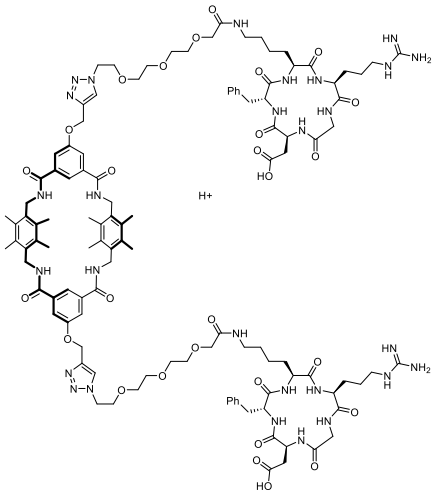

Chemical Formula: $C_{116}H_{157}N_{28}O_{28}^{+}$
Exact Mass: 2390.1717
Molecular Weight: 2391.6995
m/z: 2391.1750 (100.0%), 2390.1717 (79.7%), 2392.1784 (62.2%), 2393.1817 (16.2%), 2392.1721 (10.3%), 2393.1817 (9.3%), 2391.1687 (8.2%), 2393.1793 (5.8%), 2394.1851 (5.3%), 2392.1759 (4.6%), 2394.1826 (3.6%), 2393.1754 (3.5%), 2393.1754 (2.9%), 2394.1851 (2.5%), 2394.1788 (2.2%), 2392.1813 (1.8%), 2395.1884 (1.6%), 2391.1779 (1.4%), 2393.1846 (1.1%), 2392.1792 (1.1%)

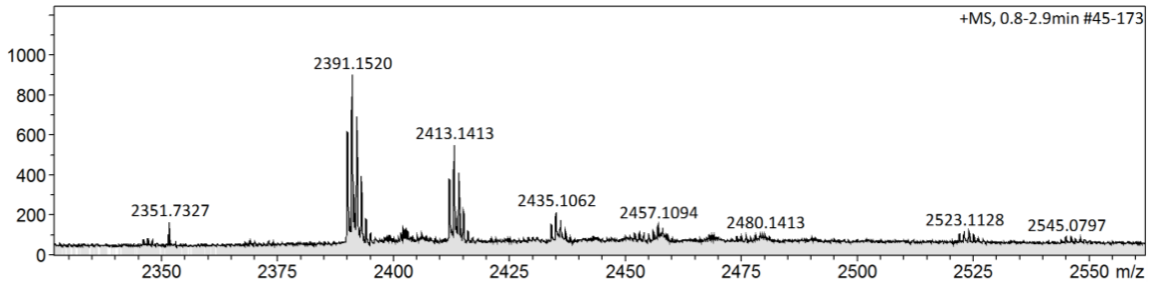

Figure S3. Compound **T** HRMS (ESI-TOF).

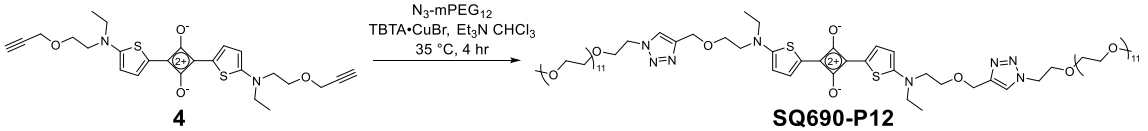

4 **SQ690-P12**

Compound **SQ690-P12.**

Compound **4** was synthesized according to a previously reported procedure.[S2] Compound **4** (21 mg, 0.042 mmol), $mPEG_{12}$-N_3 (58 mg, 0.100 mmol), triethylamine (4 drops), and TBTA•CuBr (4 mg) were mixed in $CHCl_3$ (5 mL). The reaction mixture was sonicated at 40 ˚C for 4 h. The solvent was then removed by rotary evaporation, and the residue was purified by column chromatography (silica, 0-20% MeOH/$CHCl_3$) to obtain the product

SQ690-P12 as dark blue solid (22 mg, 32%). **^{1}H NMR** (400 MHz, $(CD_3)_2CO$): δ 7.87 (s, 2H), 7.73 (s, 2H), 6.41 (s, 2H), 4.51 (s, 4H), 4.43 (s, 4H), 3.74 (s, 8H), 3.67 (s, 4H), 3.55 (s, 4H), 3.44 (s, 88H), 3.34 (s, 4H), 3.16 (s, 6H), 1.17 (s, 6H). **HRMS (ESI-TOF)**: calculated for $C_{76}H_{130}N_8O_{28}S_2^+$ $[M+H]^+$ 1667.8509, found 1667.8507.

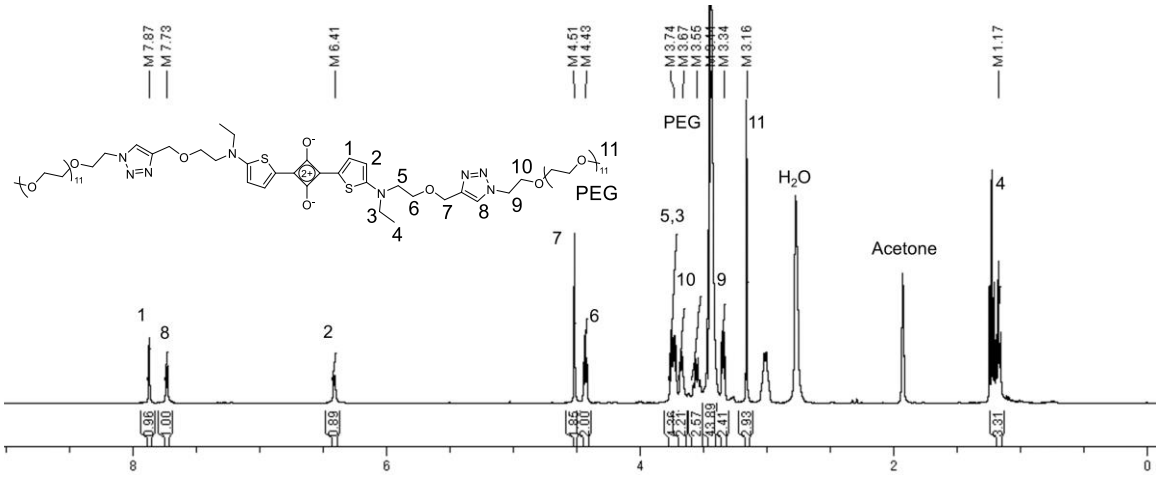

Figure S4. Compound **SQ690-P12** ^{1}H NMR Spectrum (400 MHz, $(CD_3)_2CO$).

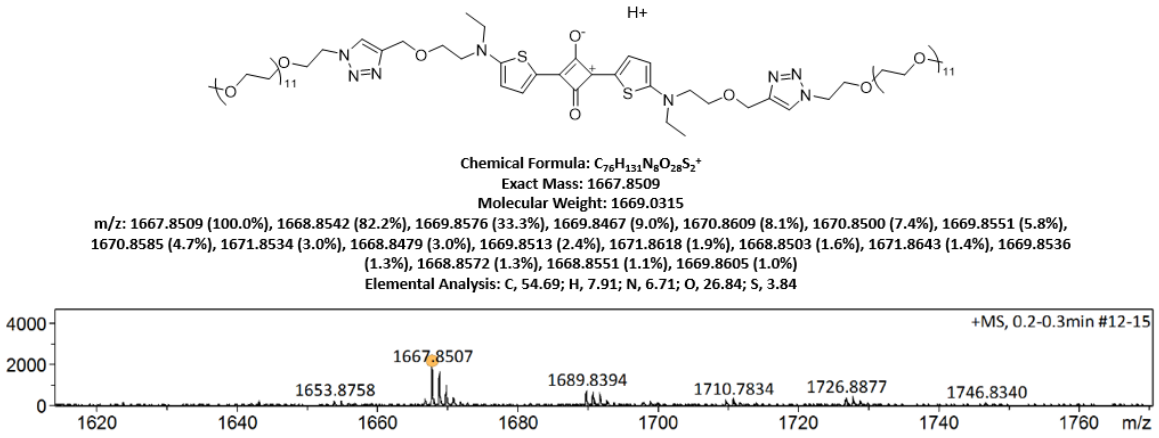

Figure S5. Compound **SQ690-P12** HRMS (ESI-TOF).

B. Probe Pre-assembly Characterization

Absorbance and Fluorescence Studies

Absorption spectra were collected on Evolution 201 UV/Vis Spectrometer with Thermo Insight software. Fluorescence spectra were acquired using a Horiba Fluoromax-4 Fluorometer with FluorEssence software. Spectra were obtained for **SQ690** and **SQ830** dyes (3.0 μM) using deionized water at 20 ℃ with 1- or 3-mL quartz cuvette (1 cm path length). One molar equivalent of **C** or **T** was then added, and the absorption and fluorescence spectra were collected again. Complexation was confirmed by a red shift in absorption and emission maxima as well as a six-fold increase in fluorescence intensity. Molar absorptivities were determined for the dyes and the pre-assembled probes at 3.0 μM in deionized water. Quantum yield measurement was calculated relative to methylene blue (Φ_f = 0.02 in H_2O)[S5] for the **SQ690** dyes and the **SQ690** pre-assembled probes. Quantum yield measurement was calculated relative to indocyanine green (Φ_f = 0.053 in H_2O)[S3] for the **SQ830** dye and the **SQ830** pre-assembled probe. For the quantum yield of the dyes, the absorbance of 0.08 was used relative to the standard dyes (methylene blue or indocyanine green). For the pre-assembled probes, a stock solution using 2:1 molar ratio of macrocycle to dye at 100 μM was prepared. An absorbance of 0.08 of the pre-assembled probes were then used relative to the standard dyes (methylene blue or indocyanine green). All measurements were done in triplicate.

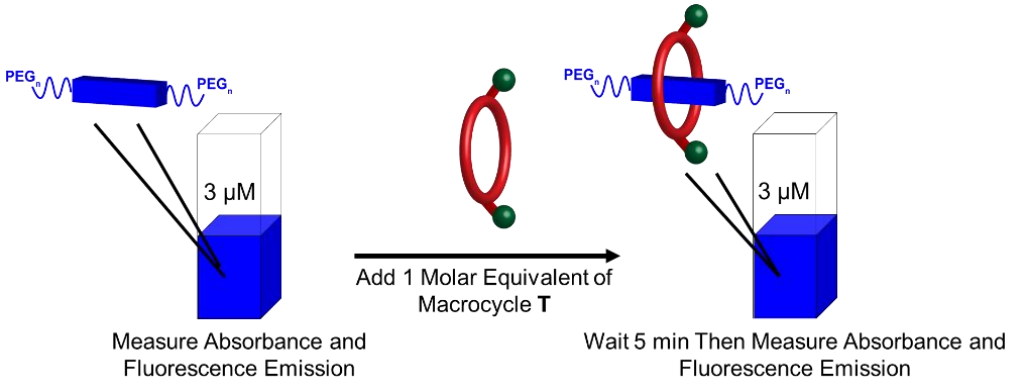

Scheme S1. Schematic of probe pre-assembly process to confirm complexation

Table S1. Photophysical properties of free dye and pre-assembled complexes in water at 3 μM.

Compound	MW (g/mol)	λ_{abs} (nm)	λ_{em} (nm)	log ε	Φ_f[a]
SQ690-P3	847.02	660	678	5.450	0.04
C ⊃ SQ690-P3	2320.53	663	690	5.393	0.22
T ⊃ SQ690-P3	3237.71	663	691	5.382	0.15[b]
SQ690-P12	1668.03	662	679	5.433	0.02
C ⊃ SQ690-P12	3141.54	665	691	5.361	0.21
T ⊃ SQ690-P12	4058.72	665	694	5.310	0.16
SQ690-P45	4575.52	663	679	5.377	0.03
C ⊃ SQ690-P45	6049.04	668	689	5.250	0.13
T ⊃ SQ690-P45	6966.21	670	693	5.069	0.12
SQ830-P45	4687.69	796	819	5.173	0.07
C ⊃ SQ830-P45	6161.20	804	830	5.242	0.10

[a] Φ_f was calculated using a 2:1 molar ratio of macrocycle to dye where excess macrocycle induced a small quenching effect that is not observed with dye alone
[b] Φ_f was approximated using a 1:1 molar ratio of macrocycle to dye

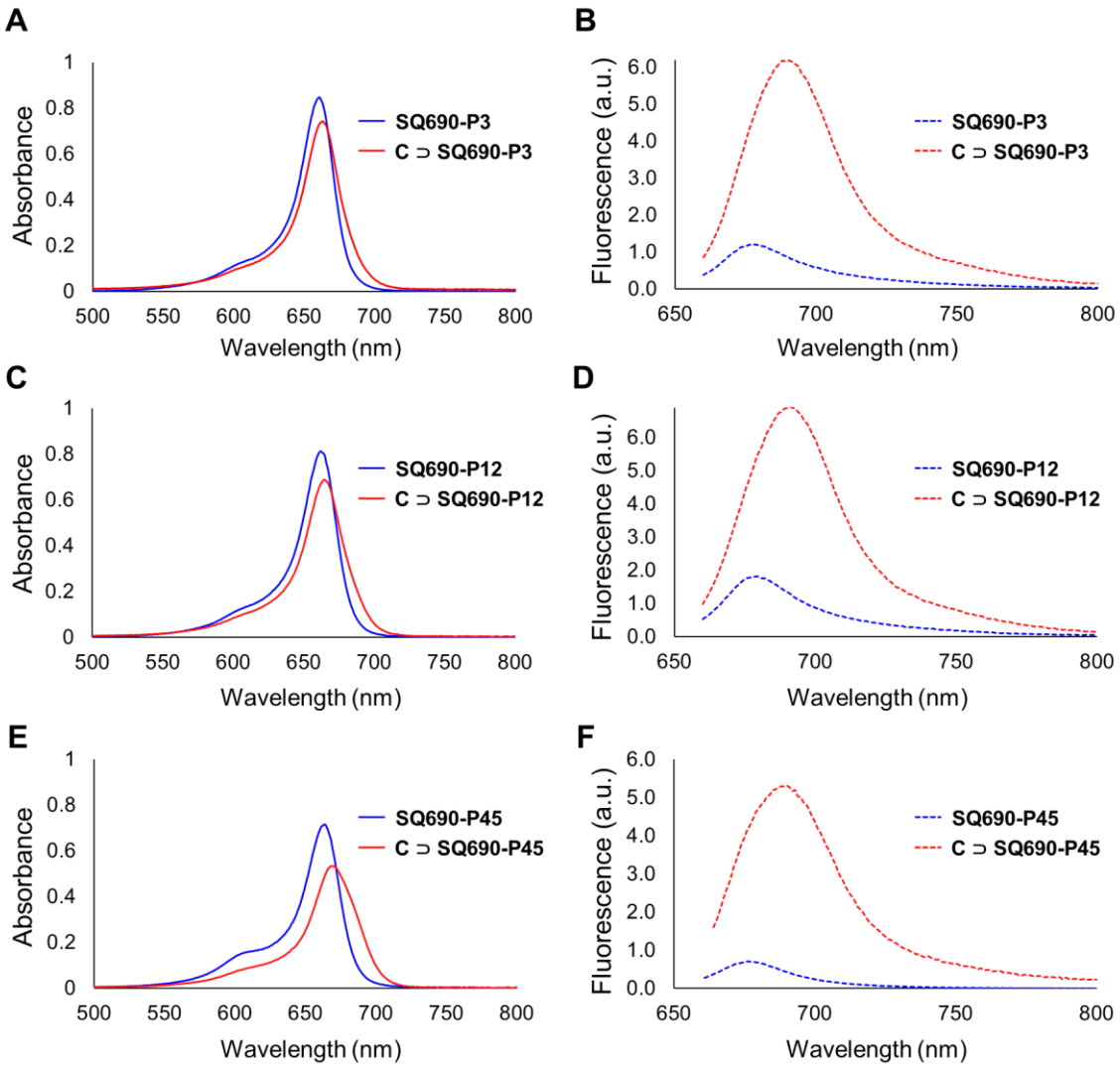

Figure S6. Absorbance and emission spectra of pre-assembled probe and its corresponding free dye: (A,B) **C ⊃ SQ690-P3**, (C,D) **C ⊃ SQ690-P12**, and (E,F) **C ⊃ SQ690-P45**. All solutions were 3 μM in water. Fluorescence emission spectra were obtained with 650 nm excitation at 2 nm slit width.

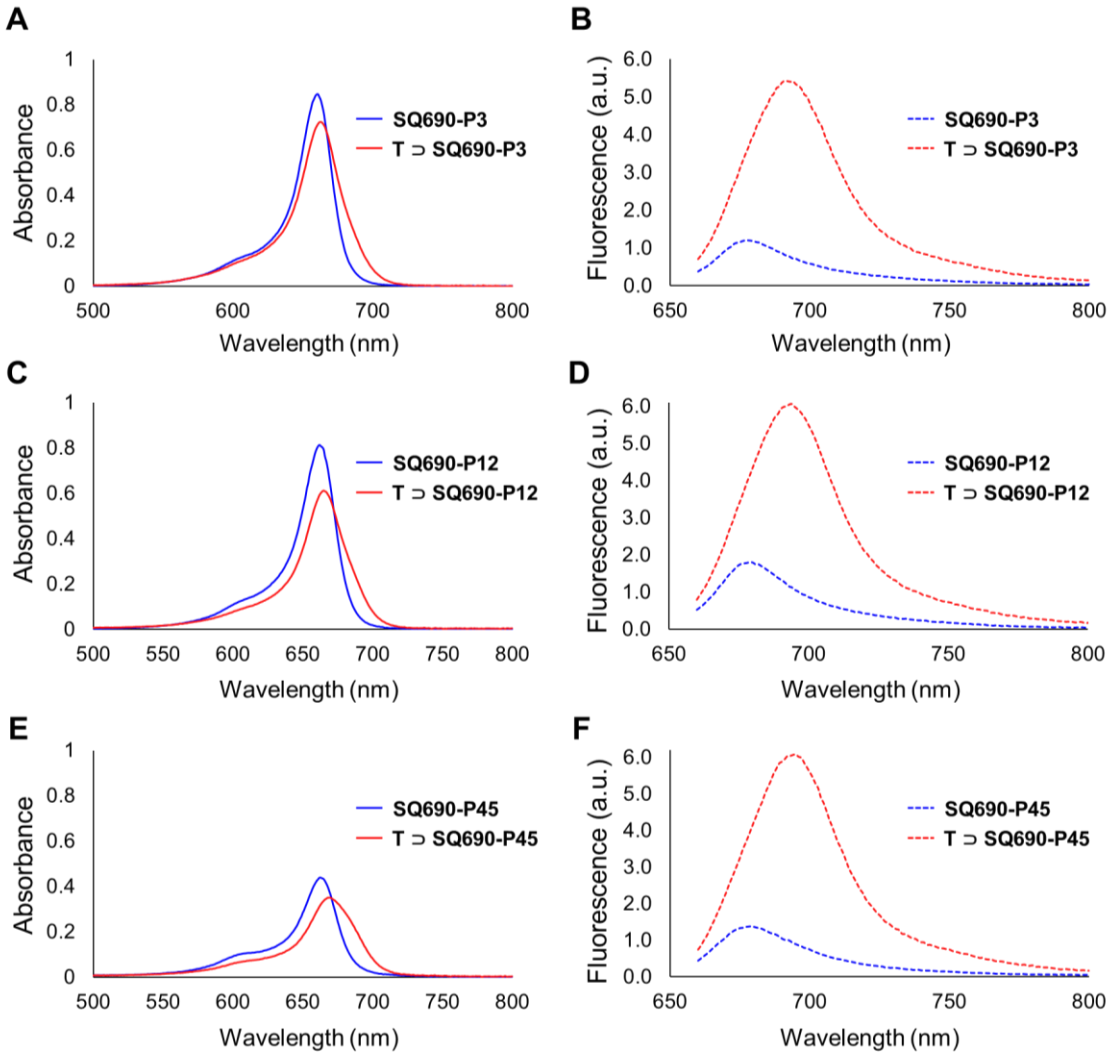

Figure S7. Absorbance and emission spectra of pre-assembled probe and its corresponding free dye: (A,B) **T ⊃ SQ690-P3**, (C,D) **T ⊃ SQ690-P12**, and (E,F) **T ⊃ SQ690-P45**. All solutions were 3 μM in water. Fluorescence emission spectra were obtained with 650 nm excitation at 2 nm slit width.

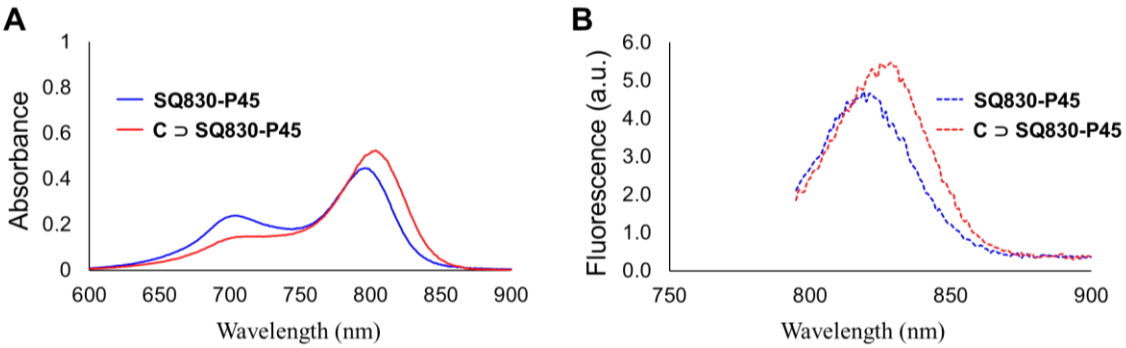

Figure S8. (A) Absorbance and (B) emission spectra of **SQ830-P45** and pre-assembled **C ⊃ SQ830-P45**. All solutions were 3 μM in water. Fluorescence emission spectra were obtained with 785 nm excitation at 3 nm slit width.

Agarose Gel Electrophoresis

Agarose gel electrophoresis was used to confirm complexation of the pre-assembled probes. The **SQ690** dyes and **C ⊃ SQ690** probes were added to separate wells in a 2.5% agarose gel (100 μM, 10 μL). Then cold TBE buffer (pH 8.3, 8.9 mM Tris, 8.9 mM borate, 200 μM) was added to cover the gel, but not the wells to prevent the compounds from leaking into the buffer. The gel was run at 100 V for 30 min to load the compounds into the gel at which time the gel was completely covered with TBE buffer and was run at 110 V for 2 h. The gel was photographed in ambient light, and a fluorescent image was acquired using the In vivo Imaging System (filter: Cy5.5, acquisition time: 3 s, binning: small, F-stop: 2, field-of-view 10 x 10 cm). For the **SQ690** dyes and **T ⊃ SQ690** probes, the procedure was repeated with a 2.25% agarose gel where the gel was run at 120 V for 3.5 hr. For the **SQ830-P45** dye and **C ⊃ SQ830-P45** probe, the samples were loaded into the wells (9 mM, 10 μL), and the gel was run with cold TBE buffer (pH 8.3, 8.9 mM Tris, 8.9 mM borate, 200 μM) at 110 V for 1.5 hr. The gel was photographed in ambient light, and a fluorescent image was acquired using Ami HT Spectral Instruments Imaging (ex: 745 nm, em: 850 nm, exposure: 3 s, percent power: 30%, F-stop: 2, binning: small). The pre-assembled probes were found to be complexed based on the differences in migration patterns and higher fluorescence intensity of the pre-assembled probes.

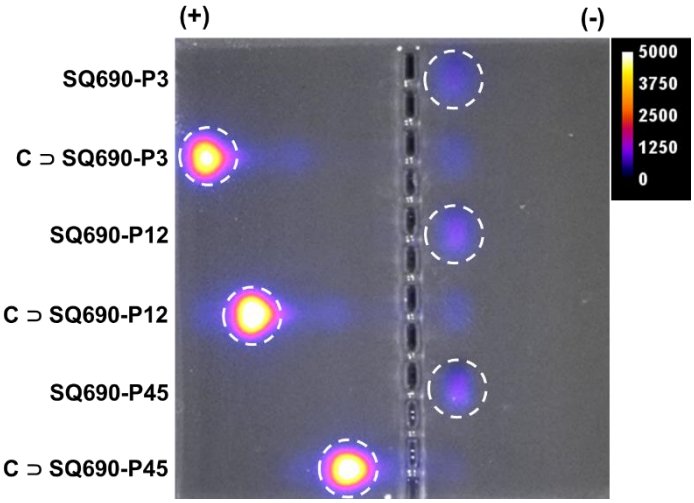

Figure S9. Agarose gel loaded with **SQ690** dyes and pre-assembled **C ⊃ SQ690** probes. The samples (100 μM/well) were run on a 2.5% agarose gel at 100 V for 30 min followed by 110 V for 1.5 h. Gels were photographed in ambient light and overlaid with a fluorescent image acquired with the in vivo imaging station (Cy5.5 filter).

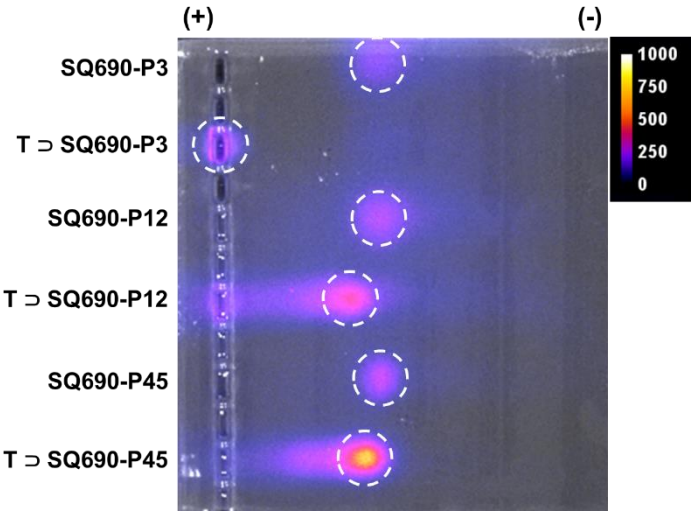

Figure S10. Agarose gel loaded with **SQ690** dyes and pre-assembled **T ⊃ SQ690** probes. The samples (100 μM/well) were run on a 2.25% agarose gel at 100 V for 30 min followed by 120 V for 3 h. Gels were photographed in ambient light and overlaid with a fluorescent image acquired with the in vivo imaging station (Cy5.5 filter).

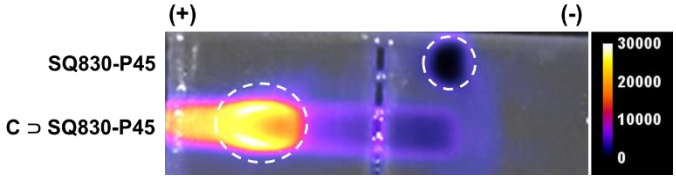

Figure S11. Agarose gel loaded with **SQ830-P45** dye and pre-assembled **C ⊃ SQ830-P45** probe. The samples (9 mM/well) were run on a 2.25% agarose gel at 100 V for 30 min followed by 110 V for 1.5 h. Gels were photographed in ambient light and overlaid with a fluorescent image acquired with in vivo imaging station (ex: 745 nm, em: 850 nm).

C. In vitro Studies

Cell Viability Studies

To measure cell toxicity of the pre-assembled **C ⊃ SQ690-P3** and **C ⊃ SQ690-P45** probes, a common MTT cell viability assay was used. CHO-K1 (Chinese hamster ovary; ATCC CCL-61) were cultured and maintained in F-12K medium (supplemented with 10% fetal bovine serum; 1% penicillin streptomycin) at 37 °C and 5% CO_2 in a humidified incubator. The CHO-K1 cells were seeded into 96-microwell plates and grown to 70% confluency. The cells were incubated with either **C ⊃ SQ690-P3** or **C ⊃ SQ690-P45** at various concentrations (N =3) in F12-K medium for 24 h at 37 °C, 5% CO_2. The medium was then removed and replaced with F-12K medium containing [3-(4,5-dimethylthiazol-2-yl)-2,5-diphenyltetrazolium bromide] (MTT, 1.1 mM). The samples were incubated for 3 h at 37 °C and 5% CO_2 and an SDS−HCl detergent solution was the added. The samples were incubated overnight, and the absorbance of each well was measured at 570 nm (N = 3), where the readings were normalized relative to untreated cells. Based on the results from the assay, neither **C ⊃ SQ690-P3** or **C ⊃ SQ690-P45** displayed cell toxicity up to 5 μM.

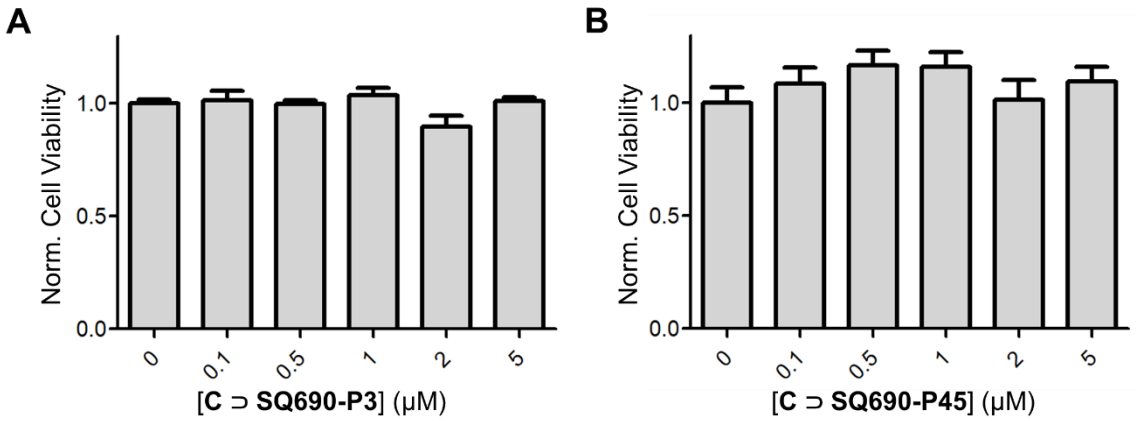

Figure S12. MTT cell viability assay. CHO-K1 Chinese hamster ovary cells were treated for 24 h at 37 °C, 5% CO_2 with either (A) **C ⊃ SQ690-P3** or (B) **C ⊃ SQ690-P45**.

Flow Cytometry Studies

Integrin expression was evaluated with EMT-6 cells (mouse mammary carcinoma, ATCC CRL-2755) using flow cytometry. EMT-6 cells were cultured and maintained in Waymouth's MB 752/1 medium (supplemented with 15% fetal bovine serum; 1% penicillin streptomycin) at 37 °C and 5% CO_2 in a humidified incubator. The EMT-6 cells were grown in a 25 cm^2 cell culture flask and were dissociated from the flask with a non-enzymatic cell dissociation solution (Sigma Aldrich). The cells were collected and aliquoted such that each 1.8 mL centrifuge tube contained $1.5x10^5$ cells. The cells were incubated for 30 min at 4 ℃ with FITC conjugated β_5 antibody (ThermoFisher Scientific, KN52, 0.375 μg/mL) in flow cytometry staining buffer (ThermoFisher Scientific). The antibody was removed, and

the cells were washed twice with flow cytometry staining buffer, fixed with IC fixation buffer (ThermoFisher Scientific), and transferred to flow cytometry tubes. Using a BD LSRFortessa X-20 flow cytometer, the cells were excited at 488 nm and emission was collected with a FITC 520/530 nm filter (max: 20,000 events). The data was then analyzed on the software package FlowJo. Flow cytometry verified that the EMT-6 cells do not express the β_5 protein subunit where there was minimal cell staining with fluorescent FITC conjugated β_5 antibody.

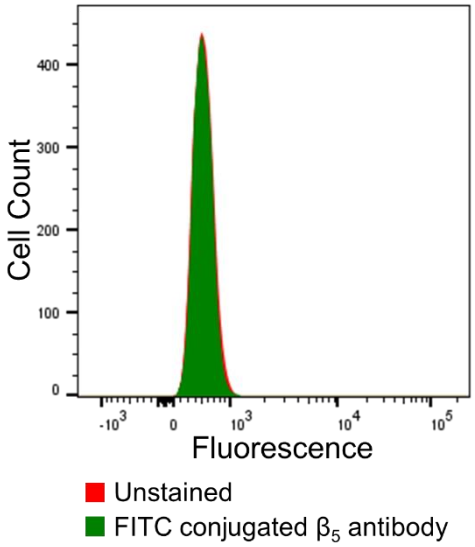

Figure S13. Flow cytometry of integrin negative EMT-6 cells. The EMT-6 cells have low β_5 expression as indicated by minimal staining with fluorescent FITC conjugated β_5 antibody.

Fluorescence Cell Microscopy Studies

Cell targeting of the pre-assembled **T ⊃ SQ690** probes was determined through fluorescence cell microscopy. OVCAR-4 cells were cultured and maintained in RPMI-1640 medium (supplemented with 10% fetal bovine serum; 1% non-essential amino acids; 1% L-glutamine; 1% penicillin streptomycin) at 37 °C and 5% CO_2 in a humidified incubator. EMT-6 cells were cultured and maintained in Waymouth's MB 752/1 medium (supplemented with 15% fetal bovine serum; 1% penicillin streptomycin) at 37 °C and 5% CO_2 in a humidified incubator. Both cell lines were seeded into 8-well chambered coverglass (Lab-Tek, Nunc, USA) and grown to 70% confluency. The cells were incubated with 1 μM probe in media for 30 min at 37℃. For blocking, 200 μM excess cRGD was added to the cells for 5 min prior to probe treatment and remained present during probe incubation. The cells were washed three times with 1xPBS, fixed with 4% cold paraformaldehyde for 20 min at room temperature, washed again with 1xPBS, and co-stained with 3 μM Hoechst 33342 for 10 min. Afterwards, the cells were washed two times

with 1xPBS and imaged on Zeiss Axiovert 100 TV epifluorescence microscope equipped with UV filter (ex. 387/11, em. 447/60) and Cy5.5 filter (ex. 655/40, em. 716/40). For each micrograph, a background subtraction with a rolling ball radius of 200 pixels was conducted using ImageJ2 software. The average mean fluorescence intensity for each micrograph was then calculated from using 20 randomly generated 25 x 25 pixel extra-nuclear ROIs. The averages and SEM were calculated and plotted in GraphPad Prism.

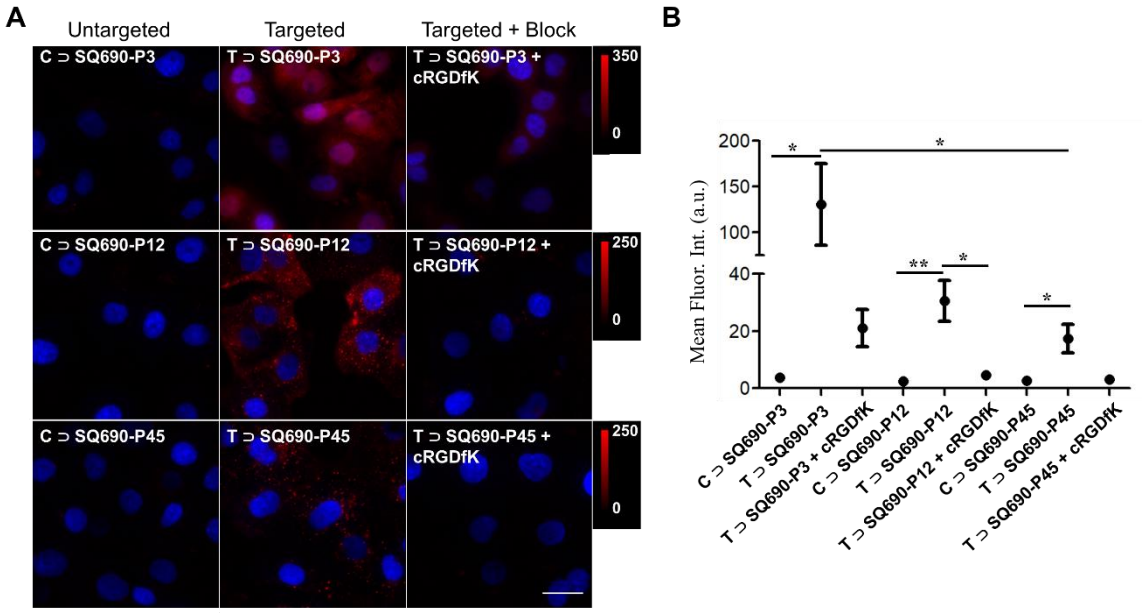

Figure S14. Targeting integrin positive OVCAR-4 cells. (A) Representative epifluorescent micrographs showing probe uptake by OVCAR-4 cells after a 30-min incubation: 1 μM **C ⊃ SQ690** (untargeted), 1 μM **T ⊃ SQ690** (targeted), or 1 μM **T ⊃ SQ690** + 200 μM cRGDfK (targeted + block). Blue fluorescence shows Hoechst nuclear stain. For each row, the calibration bar for near-infrared fluorescence intensity is in the upper right corner where units are arbitrary. Scale bar = 30 μm. (B) Quantification of intracellular mean fluorescence intensities as a measure of probe internalization. The threshold p-values are: * $p<0.05$, ** $p<0.01$, *** $p<0.001$.

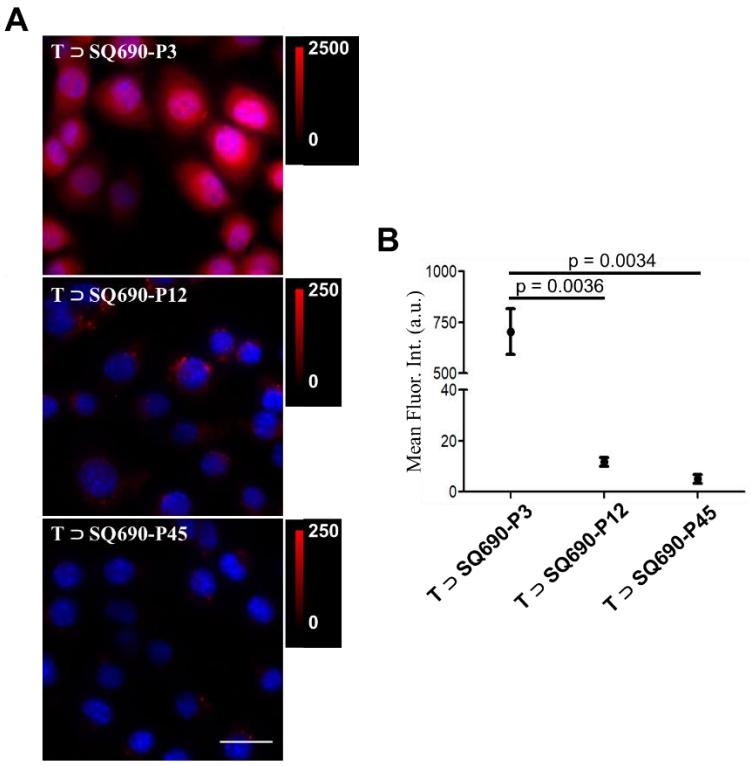

Figure S15. Integrin negative EMT-6 cells with pre-assembled **T ⊃ SQ690** probes (A) Representative epifluorescent micrographs of integrin negative EMT-6 cells after a 30-min incubation with targeted probe. Blue fluorescence shows Hoechst nuclear stain. For each row, the calibration bar for near-infrared fluorescence intensity is in the upper right corner where units are arbitrary. Scale bar = 30 μm. (B) Quantification of intracellular mean fluorescence intensities as a measure of probe internalization. P-values with statistical significance are shown on the plot.

D. In vivo Studies: Single Agent Imaging

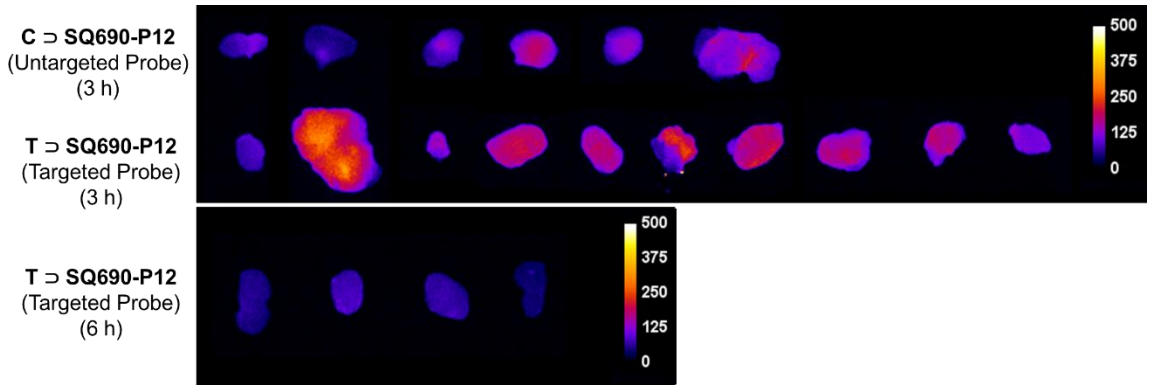

Figure S16. Near-infrared fluorescent images of excised tumors from mice used in single agent imaging at 3 h and 6 h post-injection. Mice received an intravenous injection of **C ⊃ SQ830-P12** (untargeted probe) or **T ⊃ SQ690-P12** (targeted probe) (10 nmol/mouse).

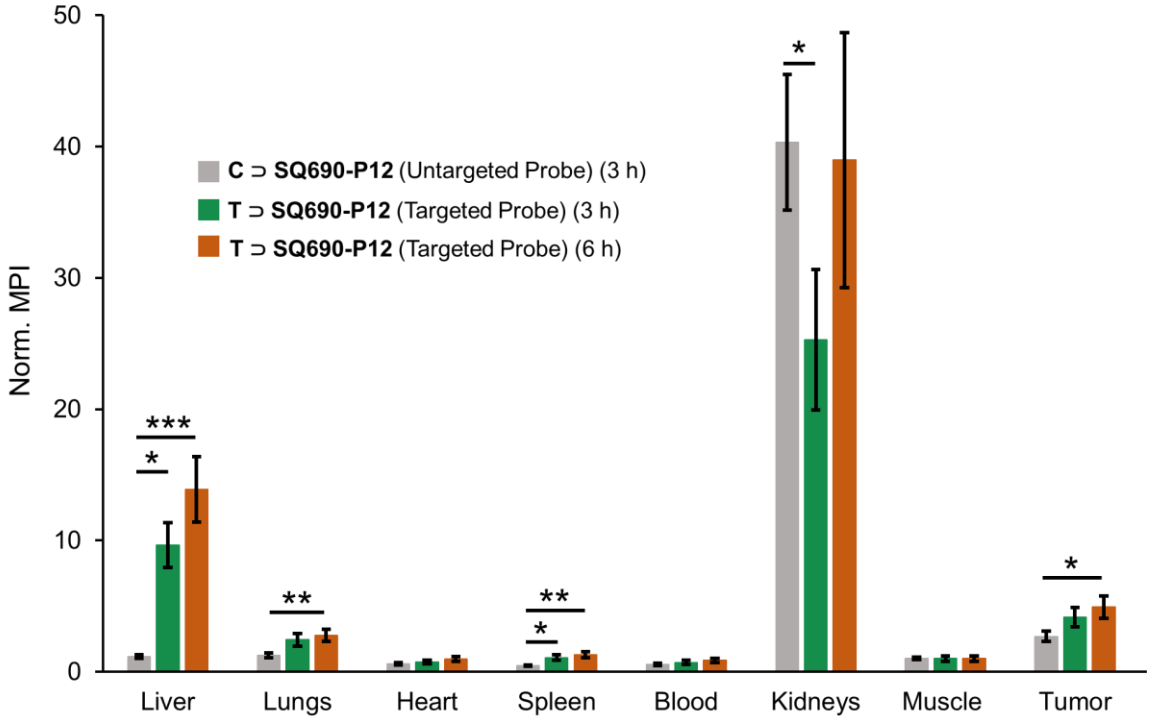

Figure S17. Mouse biodistribution of fluorescent probes in single agent imaging with injection of either **C ⊃ SQ630-P45** (untargeted) in cohort 1 or **T ⊃ SQ690-P45** (targeted) in cohort 2. The mean pixel intensity (MPI) for each resected organ is relative to the MPI for thigh muscle from the same animal; error bars indicate ±SEM. The threshold p-values are: * $p<0.05$, ** $p<0.01$, *** $p<0.001$.

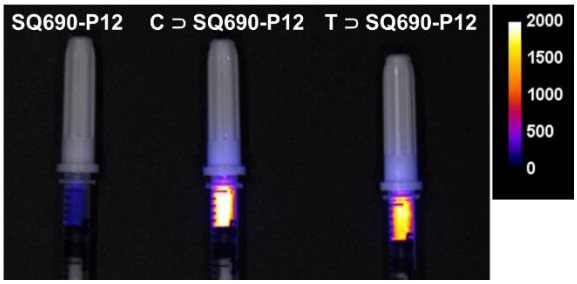

Figure S18. Comparison of fluorescent probe images acquired using the same parameters for animal imaging using the in vivo imaging station (Filter: Cy5.5, Acquisition time: 3 s, Binning: small, F-stop: 2, Field-of-view 10 x 10 cm). Shown from left to right in aqueous solution (5 μM): **SQ690-P12**, **C ⊃ SQ690-P12**, **T ⊃ SQ690-P12**. The images indicate that the IVIS signal intensity for the free dye **SQ690-P12** is 4 times weaker than the pre-assembled probes.

E. In vivo Studies: Paired Agent Imaging

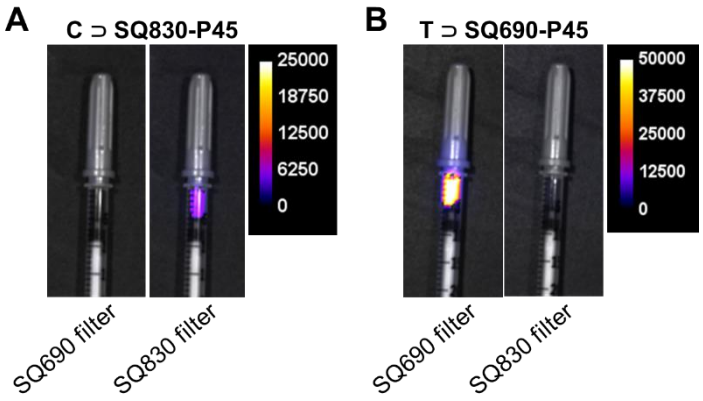

Figure S19. Comparison of fluorescent probe images acquired in two different filter sets using the same parameters for animal imaging using the in vivo imaging station [SQ690 (ex: 640 nm, em: 710 nm, exposure: 3 s, percent power: 50%, F-stop: 2, binning: small) and SQ830 (ex: 745 nm, em: 850 nm, exposure: 3 s, percent power: 30%, F-stop: 2, binning: small)]. In aqueous solution (200 μM), right image is taken in the SQ830 filter set, and left image is taken in the SQ690 filter. (A) **C ⊃ SQ830-P45** (B**) T ⊃ SQ690-P45**. The images indicate that with these parameters each probe is only visualized in their respective filter set.

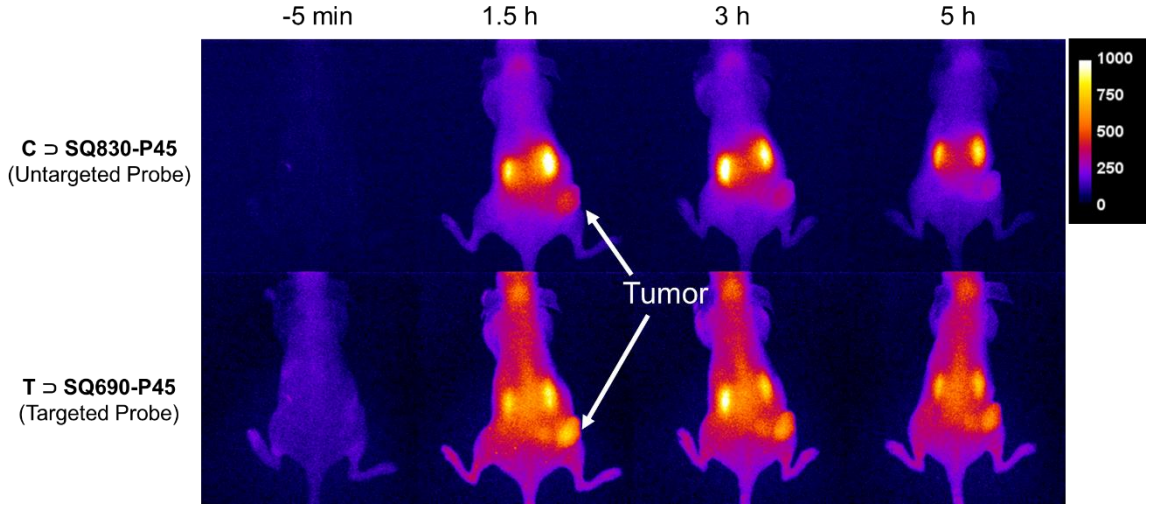

Figure S20. Representative fluorescent images of tumor-burdened mice used in paired agent imaging. Mice received intravenous co-injection of **C ⊃ SQ830-P45** (untargeted) and **T ⊃ SQ690-P45** (targeted) (20 nmol/mouse). Images were taken at -5 min, 1.5 h, 3 h, and 5 h after injection. Mice were imaged in two different filter sets using the in vivo imaging station [SQ690 (ex: 640 nm, em: 710 nm, exposure: 3 s, percent power: 50%, F-stop: 2, binning: small) and SQ830 (ex: 745 nm, em: 850 nm, exposure: 3 s, percent power: 30%, F-stop: 2, binning: small)].

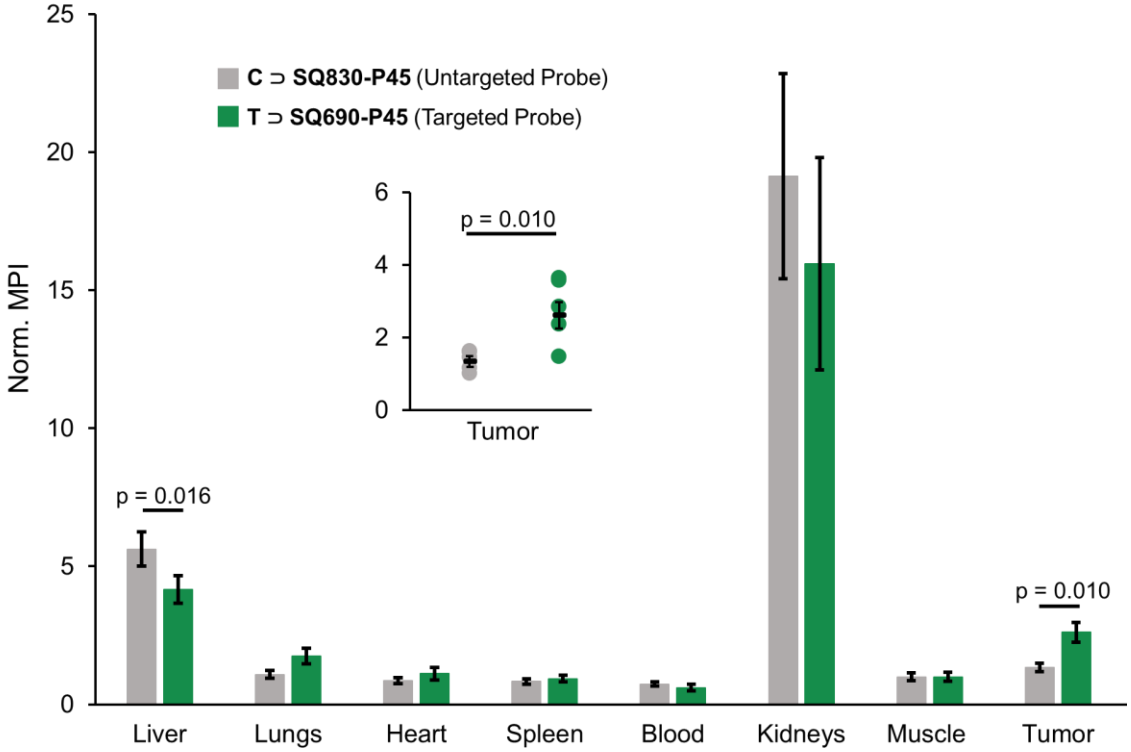

Figure S21. Mouse biodistribution of fluorescent probes in paired agent imaging with co-injection of pre-assembled **C ⊃ SQ830-P45** (untargeted) and **T ⊃ SQ690-P45** (targeted) probes. The mean pixel intensity (MPI) for each resected organ is relative to the MPI for thigh muscle from the same animal; error bars indicate ±SEM. Insert shows scatter plot for normalized tumor MPI data. P-values with statistical significance are shown on the plots.

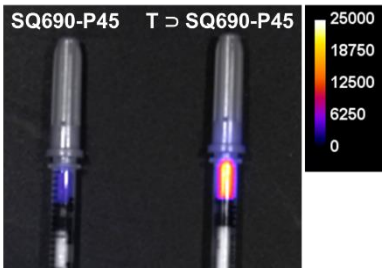

Figure S22. Comparison of fluorescent probe images acquired using the same parameters for animal imaging using the in vivo imaging station (ex: 640 nm, em: 710 nm, exposure: 3 s, percent power: 50%, F-stop: 2, binning: small). In aqueous solution (5 μM), right image is free dye **SQ690-P45**, and the left image is **T ⊃ SQ690-P45**. The images indicate that signal intensity for the free dye **SQ690-P45** is 4 times weaker than the pre-assembled probe.

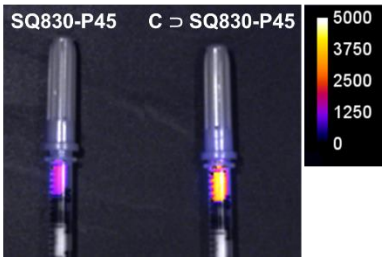

Figure S23. Comparison of fluorescent probe images acquired using the same parameters for animal imaging using the in vivo imaging station (ex: 745 nm, em: 850 nm, exposure: 3 s, percent power: 30%, F-stop: 2, binning: small)]. In aqueous solution (5 μM), right image is free dye **SQ830-P45**, and the left image is **C ⊃ SQ830-P45**. The images indicate that signal intensity for the free dye **SQ830-P45** is 4 times weaker than the pre-assembled probe.

References

(1) Dempsey, J. M., Zhai, C., McGarraugh, H. H., Schreiber, C. L., Stoffel, S. E., Smith, B. D., Johnson, A., Smith, B. D. (2019) High Affinity Threading of New Tetralactam Macrocycle in Water by Fluorescent Deep-Red and near-Infrared Squaraine Dyes. *Chem. Commun. 55*, 12793–12796.

(2) Peck, E. M., Liu, W., Spence, G. T., Shaw, S. K., Davis, A. P., Destecroix, H., Smith, B. D. (2015) Rapid Macrocycle Threading by a Fluorescent Dye−Polymer Conjugate in Water with Nanomolar Affinity. *J. Am. Chem. Soc. 137*, 8668–8671.

(3) Liu, W., McGarraugh, H., Smith, B. (2018) Fluorescent Thienothiophene-Containing Squaraine Dyes and Threaded Supramolecular Complexes with Tunable Wavelengths between 600–800 Nm. *Molecules 23*, 2229.

(4) Shaw, S. K., Liu, W., Gomez-Duran, C. F. A., Schreiber, C. L., Betancourt-Mendiola, M. de L., Zhai, C., Roland, F. M., Padanilam, S. J., Smith, B. D. (2018) Non-Covalently Pre-Assembled High-Performance near-Infrared Fluorescent Molecular Probes for Cancer Imaging. *Chem. - A Eur. J. 24*, 13821–13829.

(5) Atherton, S. J., Harriman, A. (1993) Photochemistry of Intercalated Methylene Blue: Photoinduced Hydrogen Atom Abstraction from Guanine and Adenine. *J. Am. Chem. Soc. 115*, 1816–1822.